

UHASSELT



Maastricht University

KNOWLEDGE IN ACTION

## Faculty of Medicine and Life Sciences School for Life Sciences

Master of Biomedical Sciences

### Master's thesis

**Acyl-CoA-binding protein (ACBP) deletion in brown adipose tissue impairs high-fat diet-induced cardiac remodeling**

#### Niki Sciarrino

Thesis presented in fulfillment of the requirements for the degree of Master of Biomedical Sciences, specialization Molecular Mechanisms in Health and Disease

#### SUPERVISOR :

Prof. dr. Virginie BITO

#### SUPERVISOR :

Prof. dr. Ana PLANAVILA

#### MENTOR :

Albert BLASCO ROSET

Transnational University Limburg is a unique collaboration of two universities in two countries: the University of Hasselt and Maastricht University.



UHASSELT

KNOWLEDGE IN ACTION

[www.uhasselt.be](http://www.uhasselt.be)  
Universiteit Hasselt  
Campus Hasselt:  
Martelarenlaan 42 | 3500 Hasselt  
Campus Diepenbeek:  
Agoralaan Gebouw D | 3590 Diepenbeek

2023  
2024



**UHASSELT**

KNOWLEDGE IN ACTION



**Maastricht University**

# **Faculty of Medicine and Life Sciences**

## ***School for Life Sciences***

Master of Biomedical Sciences

### ***Master's thesis***

***Acyl-CoA-binding protein (ACBP) deletion in brown adipose tissue impairs high-fat diet-induced cardiac remodeling***

**Niki Sciarrino**

Thesis presented in fulfillment of the requirements for the degree of Master of Biomedical Sciences, specialization Molecular Mechanisms in Health and Disease

### **SUPERVISOR :**

Prof. dr. Virginie BITO

### **SUPERVISOR :**

Prof. dr. Ana PLANAVILA

### **MENTOR :**

Albert BLASCO ROSET



## Acyl-CoA-binding protein (ACBP) deletion in brown adipose tissue alters high-fat diet-induced cardiac remodeling

Niki Sciarrino<sup>1,2</sup>, Albert Blasco Roset<sup>1</sup>, Artur Navarro<sup>1</sup>, Francesc Villarroya<sup>1</sup>, and Anna Planavila<sup>1</sup>

<sup>1</sup>Departament de Bioquímica i Biologia Molecular, Institut de Biomedicina, Universitat de Barcelona, Barcelona, Spain

<sup>2</sup>UHasselt – Hasselt University, Faculty of Medicine and Life Sciences, Agoralaan, 3590 Diepenbeek, Belgium

*BAT's ACBP deletion and cardiac function upon HFD*

To whom correspondence should be addressed: Anna Planavila, Tel: +34 934021210; Email: [aplanavila@ub.edu](mailto:aplanavila@ub.edu); Niki Sciarrino, Tel +32 474040809; Email: [niki.sciarrino@student.uhasselt.be](mailto:niki.sciarrino@student.uhasselt.be)

**Keywords:** Acyl-CoA-binding protein, Brown adipose tissue, heart, obesity, fibrosis, hypertrophy

### ABSTRACT

Cardiovascular disease (CVD) is the leading cause of death worldwide. Researchers have found that factors secreted by the brown adipose tissue (BAT) can influence heart function. One of those factors is acyl-CoA binding protein (ACBP), a secretable protein involved in lipid metabolism that links fatty acyl-CoA esters to metabolic pathways. This protein is therefore easily disrupted during metabolic disorders such as obesity. The current study aims to examine the cardiac effects of the specific lack of the secretable ACBP protein in brown adipocytes during high fat-diet (HFD)-induced obesity. Specific BAT-Acbp-KO mice and control Acbp Flox mice were fed a chow diet or HFD for 12 weeks before cardiac tissue was analyzed. Gene expression and protein quantification analyses of the heart were performed. Additionally, macrophages were treated with ACBP *in vitro*. Although the heart weight/tibia length (HW/TL) ratio was higher in the HFD groups for both genotypes, the genes associated with cardiac dysfunction were only induced in the BAT-Acbp-KO mice. Conversely, a reduction of fibrosis was seen in the BAT-Acbp-KO group subjected to an HFD. Moreover, the HFD BAT-Acbp-KO group showed an increase in glycolytic genes and altered fatty acid metabolism. Lastly, ACBP promoted a pro-inflammatory phenotype in macrophages *in vitro* and deletion of ACBP in BAT reduced inflammation in the heart. This study shows that a specific lack of ACBP in BAT impacts the myocardium under HFD conditions.

### INTRODUCTION

The heart is in charge of delivering nutrients, gases, and endocrine factors to all organs in the body (1). Due to this significant role, it is unsurprising that cardiovascular disease (CVD) is the leading cause of death worldwide, with around 17,9 million deaths each year (2). Some of the main risk factors for the development of CVD are smoking, a sedentary lifestyle, diabetes, hypertension, and obesity (3). Obesity and CVD are strongly associated because of the coronary risk factors that come with obesity. However, it also exerts direct effects on the heart. Except for the increased risk for heart failure that people with obesity exhibit, left ventricular hypertrophy and fibrosis also have been documented among these cases (4). However, specific

pathophysiologic pathways are yet to be investigated (5). Cardiac fibrosis is described as the uncontrolled accumulation of extracellular matrix (ECM) in the heart by the activation of fibroblasts into myofibroblasts (6). ECM deposition is usually a protective mechanism due to its crucial role in repair and wound healing. Besides, the interaction between cardiomyocytes and ECM is of great importance because of proliferation, migration, and survival signaling (7). On the contrary, pathological cardiac ECM accumulation causes a deformation in organ structure and alters cardiac function. The contractile and filling capacities of the heart are also impaired because of fibrotic turnover (8). Metabolic dysfunctions, often associated with

obesity, activate fibrogenic pathways inducing fibrotic cardiac remodeling (9). This remodeling often results in reduced ejection fraction due to increased myocardial stiffness and it eventually leads to diastolic dysfunctions (10, 11). Another process of cardiac remodeling includes the increase of the left ventricular (LV) wall leading to a decrease in contractility. This process is called cardiac hypertrophy and is characterized by an enlargement of the cardiomyocytes (12, 13). Initially, cardiac hypertrophy serves as a response to many external factors, including hypertension, contractile abnormalities, and valvular heart disease. However, prolonged cardiac hypertrophy leads to cardiomyocyte apoptosis and dysregulations, resulting in heart failure (14). Two types of hypertrophy can be defined: physiological and pathologic. Regardless of the same origin as a response to increased cardiac stress, they vary in prognosis and outcome. Physiological hypertrophy will maintain its cardiac function over time, while pathological hypertrophy has adverse cardiac outcomes, including heart failure, arrhythmias, etc., (13). Fat accumulation in obesity requires an increased workload and cardiac output (CO), and eventually an enlargement of the LV to cardiac dysfunction. Simultaneously, dyslipidemia causes induction of inflammatory responses, contributing to the pathological features of cardiac hypertrophy (15). Obesity triggers a general microinflammatory state in which the heart is also generally affected (16). Inflammation is a response to cardiac injury and activates many mechanisms for tissue repair. However, uncontrolled inflammation can worsen cardiac function and induce hypertrophy, fibrosis, and hypertension (17). Cardiac inflammation is mainly controlled by monocytes/macrophages (18). Residential macrophages often have an M2 or anti-inflammatory phenotype. However, during obesity, a switch to M1 macrophages occurs due to the alternations in hormones, metabolic substrates, mechanical stress, and residential inflammatory molecules (17). M1 macrophages secrete pro-inflammatory cytokines and act as key regulators of the processes mentioned before (16). Furthermore, they can control cardiac fibrosis by signaling fibroblasts and activating them into myofibroblasts (18). Although M1 macrophages recruit myofibroblasts for the initiation of repair mechanisms in cardiac injury, chronic inflammation leads to excessive ECM production, promoting cardiac damage (19).

Fatty acids are the most efficient energy substrates (20). Given the high energy consumption that the heart requires for its function, adapting to changes in lipid metabolism is necessary (12, 13). The main adenosine triphosphate (ATP) source of the heart is mitochondrial oxidative phosphorylation (95%) and the remaining 5% is due to glycolysis (21). Fatty acids are accountable for 40-60% of ATP production in the heart. The fatty acids are taken up into cardiomyocytes using transporters and fatty acid-binding proteins. Once inside, they are transported into the mitochondria (22, 23). The hypertrophic heart reduces its fatty acid metabolism and increases glycolysis resulting in this active changing of the myocardium (21). This metabolic shift resembles a characteristic fetal cardiac phenotype in mice (14, 21, 22). The upregulation of glucose metabolism reduces the myocardial oxygen utilization per mole of produced ATP (14).

Acyl-coenzyme A binding protein (ACBP), also known as diazepam-binding inhibitor (DBI), has emerged as a novel target in CVD (24, 25). This protein is phylogenetically conserved and is expressed in plants, fungi, animals, and even some eubacteria. ACBP has a dual function and shows high similarity between the *Homo Sapiens* and *Mus Musculus* species (Figure S1) (26). It was first discovered for its extracellular interaction with the gamma-aminobutyric acid (GABA)-A receptor in the brain. This GABA-A receptor is triggered by GABA, which has a depressant role in the central nervous system. ACBP is an endogenous benzodiazepine secreted by neurons as a neuropeptide, which modulates the GABA-A receptor activity (27, 28). Later, its role in lipid metabolism was described, where cytosolic ACBP binds preferentially long-chain acyl coenzyme (CoA) esters, referred to as activated fatty acids (25, 28). The binding with ACBP allows the activated lipids to be coupled to different metabolic pathways (Figure S2) (29). Therefore, ACBP is involved in many neurological and metabolic processes (30).

Recently, it has been described that ACBP can be secreted peripherally in an autophagy-dependent trend, and it also influences the autophagic status of the cells in an endocrine way (29). Autophagy refers to cellular processes for degradation and recycling of intracellular components and thus maintaining cellular homeostasis (31). Different autophagic stimuli such as starvation trigger ACBP release, which in turn inhibits extracellularly the autophagic flux of

the cells as negative feedback. Moreover, ACBP treatment *per se* has been proven to block starvation-induced autophagy. Lastly, extracellular ACBP has a direct impact on metabolism. High plasmatic ACBP levels induce hyperphagy, reducing glycemia and fat accumulation. This brings the hypothesis of a negative feedback loop where fasting induces an autophagy-dependent increase of circulant ACBP levels and therefore functions as a mediator to restore food intake and inhibit autophagy (27, 29). These effects have been recently proven to be performed through the GABA-A receptor peripherally (32).

Interestingly, current research observed a positive correlation between ACBP plasma concentrations and age or BMI in humans (32). On the contrary, the ACBP levels are decreased in patients suffering from anorexia nervosa (33). Additionally, the influence of ACBP levels on many human malignant diseases has been suggested by several studies. Breast cancer patients with high ACBP mRNA levels had a negative prognostic impact on survival and progression of the disease (34). ACBP was also highly detected in colon adenocarcinoma compared with normal control tissue (35). Similarly, a high ACBP expression was seen in glioma and glioblastoma, bladder cancer stem cells, and non-small cell lung cancers (36-38). Elevated plasma levels of ACBP contribute to an increase in CVD risk in healthy individuals (24). Moreover, upon neutralizing ACBP, a reduction in fibrosis, inflammation, and cell damage was found in the heart, liver, and lungs by activating autophagic pathways. Overall, ACBP affects many cellular processes and various organs (21).

As mentioned before, ACBP has an important role in fatty acid metabolism, which is

a crucial process in all tissues, including the brown adipose tissue (BAT) (39). Preliminary data from our laboratory in mice showed the most prominent expression of ACBP was in adipose tissues, concretely in BAT (Figure 1). In this tissue, efficient activation and transfer of fatty acids are critical for proper thermogenesis (40). The BAT is the main site for non-shivering thermogenesis (41). Specifically, brown adipocytes produce heat through a proton leak caused by Uncoupling protein 1 (UCP1) instead of energy in the form of ATP. Its main metabolic source of thermogenesis is mainly free fatty acids for mitochondrial  $\beta$ -oxidation (42). To maintain this source for oxidation, the BAT uses plasmatic triglycerides and alternatively glucose (39, 42). The role of ACBP in this process is coupling long-chain fatty acids to the mitochondria for  $\beta$ -oxidation (25, 28, 43). Through the promotion of energy expenditure in this process, BAT activity is known to protect against obesity (44). This BAT activity also prevents type II diabetes and maintains glucose and insulin homeostasis in an obesity model (45, 46). Concerning the effect of a high fat diet and thus the development of obesity on lipid metabolism, an increase in circulating ACBP was found in an HFD rat model (47). Another study suggested a depletion of ACBP as a treatment for obesity because of the abnormally elevated levels in people suffering from obesity.

Recent studies have found that BAT has an influence on cardiac metabolic health by burning glucose-derived fatty acids and triglycerides (39, 48). The association between obesity and CVD has gained considerable interest since obesity is a crucial risk factor for CVD (21, 49). Disordered glucose and lipid metabolism are involved in the development of obesity, which therefore

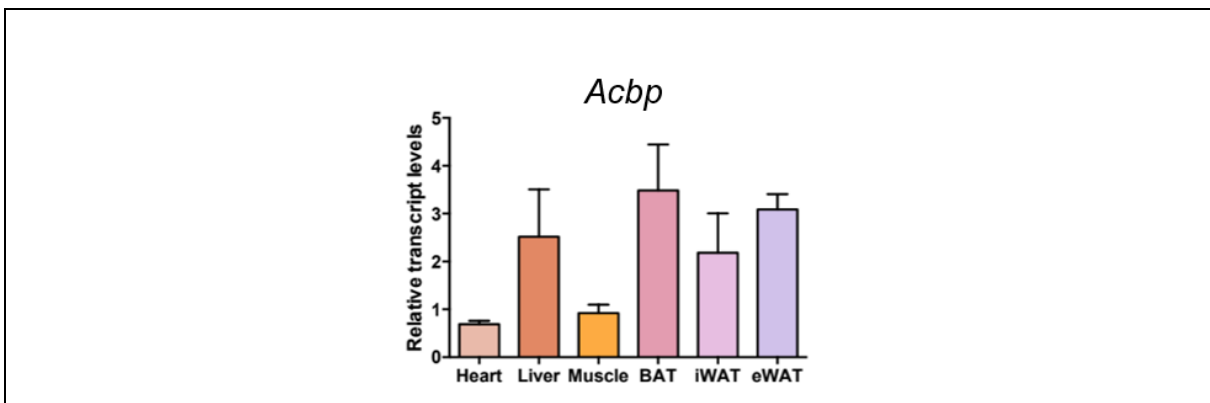


**Figure 1: Relative *Acbp* expression among different organs.** Preliminary data investigating the relative *Acbp* mRNA levels among different tissues in mice. Results are presented as the mean  $\pm$  SEM (n=4). *eWAT*, epididymal white adipose tissue; *iWAT*, inguinal white adipose tissue.

increases the possibility of developing CVD (39, 42). The prevalence of obesity is increasing globally, with 4.72 million deaths every year, where more than 70% of deaths are caused by CVD (50, 51). Obesity causes changes in lipid metabolism including a rise in lipolysis and circulating free fatty acids, insulin resistance, inflammation, and an increase in very low-density lipoprotein (52). Therefore, BAT has been targeted as a novel target against the development of obesity. During obesity, a depletion in the activity of the BAT has been found in humans, which can affect CVD (53). A negative correlation between BAT and CVD was observed in a clinical study (54). Further studies led to the discovery of hypertension, hypertrophy, and fibrosis in the heart in mice with a reduced BAT function (48, 55).

## EXPERIMENTAL PROCEDURES

*Animals* - For the generation of brown adipose tissue-specific ACBP knockout mice (BAT-Acbp-KO mice), *Acbp* flox/flox mice which were gently provided by Nils Faergeman (University of Southern Denmark; loxP sites flanking *Acbp* exon 1) and were crossed with constitutive UPC1-Cre mice (Jackson Laboratory). All mice have a C57Bl/6 background. They were housed as littermates in a controlled environment with food and water supply *ad libitum* and 12h light/dark cycles at 22°C. For the induction of obesity, mice were fed a 45% HFD (Envigo, TD.06415, Indianapolis, United States) for 3 months, while a chow diet was used as a control (Figure S3). Mice were euthanized using cervical dislocation. Body weight was measured before sacrifice. Hearts were weighted and normalized to tibia length. All animal experiments were executed following the European Community Council Directive 2010/63/EU and in agreement with the institutional animal care and use committee of the University of Barcelona.

*Plasma metabolite measurement* - Plasma glucose was measured using the Accu Chek measuring device (Roche, Basel, Switzerland). Triglyceride levels were measured using the Accutrend®Plus technology (Roche, Basel, Switzerland). Plasma metabolite measurements were done after sacrifice.

Concerning the influence of secreted factors by the BAT on heart function such as ACBP, and the role of ACBP in lipid metabolism and energy balance in the heart and in BAT, a diet-induced alternation in ACBP in the BAT could lead to myocardial alternations. The role of ACBP produced in BAT on cardiac metabolism and function when subjected to an HFD has not yet been elucidated. However, since the BAT shows increased expression of ACBP in basal conditions in preliminary data, it is interesting to examine a specific BAT-Acbp-KO model to evaluate the effect on the heart. Therefore, the purpose of this study is to elucidate the potential effect of ACBP absence in a BAT-Acbp-KO obese mice model on cardiac function. Ultimately, this study could identify ACBP as a novel target for CVD in patients suffering from obesity.

*Real-Time Reverse Transcription Polymerase Chain Reaction* - Total RNA was extracted from the left ventricle of the heart using the TriPure reagent (Roche, Indianapolis, IN, United States) and the chloroform-isopropanol method. cDNA was reverse-transcribed using the High Capacity RNA-to-cDNA kit (Applied Biosystems, Foster City, CA, United States) according to the manufacturer's instructions, and a total of 0.5µg RNA was used in a 20µl volume containing the TaqMan Universal PCR Master Mix (ThermoFisher Scientific) and primers from the Assays-by-Design Gene Expression Assay Mix or Assays-on-Demand Gene Expression Assay Mix (ThermoFisher Scientific) (Table S1). The real-time qPCR reactions were conducted using the TaqMan Gene Expression Assays (ThermoFisher Scientific, Waltham, MA, United States) according to the manufacturer's instructions using the ABI 7500 Real-Time PCR system (ThermoFisher Scientific, Waltham, MA, United States). The samples were analyzed in duplicates and the mean was calculated to obtain the gene expression of interest. The total mRNA expression was calculated using the comparative method ( $2^{-\Delta CT}$ ) and Cyclophilin A (*Ppia*) as a reference gene.

*Western blot* - Proteins were extracted from the heart using ice-cold RIPA buffer including a protease inhibitor mixture (56). The concentration of the proteins was measured using

the Pierce™ BCA protein assay kit. Proteins were loaded on 12 or 15% Sodium Dodecyl Sulfate Polyacrylamide Gels (SDS-PAGE) and transferred to Immobilon-P membranes (Millipore). Membranes were blocked using 5% milk at room temperature and incubated overnight with the primary antibodies (anti-ACBP (1:2000, homemade, gently provided by Nils J. Faergeman (University of Southern Denmark)); anti-CPT1b (1:1000; ab189182; Abcam), anti-MPC1 (1:1000; ab74871; Abcam), anti-PDK4 (1:5000; ab214938; Abcam), anti-MCT4 (1:1000; ab308528; Abcam)). Next, they were incubated for one hour at room temperature with the peroxidase-conjugated secondary goat anti-rabbit antibodies (1:3000; ab6721; Abcam). Proteins were revealed with the immobilon chemiluminescent HRP substrate reagent kit (Millipore, Billerica, MA, United States) and imaged using the iBright™ Imaging System (Invitrogen, Thermo Fisher Scientific). The Ponceau staining was used as a control. Quantification of the images was performed using the iBright Analysis software.

*RAW 264.7 cell culture* - Murine RAW 264.7 macrophages purchased from ATCC were grown in RPMI-1640 medium with 10% iFBS and 1% P/S and incubated at 37°C in a 5% CO<sub>2</sub>

## RESULTS

### *Effect of ACBP deletion in BAT on metabolic parameters in HFD-subjected mice*

To confirm our BAT-Acbp-KO model, the *Acbp* gene expression of the BAT was measured and a 4-fold KO was observed for our BAT-Acbp-KO models ( $p < 0.0001$ ; Figure 2a), whereas RNAseq confirmed this with a ten-fold KO (data not shown). Moreover, an overall HFD effect was observed causing a decrease in both models ( $p < 0.0001$ ), specifically, the flox model underwent a significant decrease of *Acbp* ( $p < 0.0001$ ; Figure 2a). Similar results were obtained for the protein levels of *Acbp* in BAT (Figure 2b). BAT expresses a high amount of *Ucp1* and this plays a major role in thermogenesis. BAT *Ucp1* was assessed to check the well-determined BAT activation under HFD, ergo a proper effect of the HFD in the BAT (57). We observed a significant increase of *Ucp1* in both genotypes ( $p < 0.0001$ ; Figure 2c). The HFD significantly increased body weight in both models ( $p < 0.0001$ ; Figure 2d). The blood glucose and triglyceride levels showed an increase in our

incubator. Gene expression analyses were conducted by plating the macrophages at  $2 \times 10^5$  cells·mL<sup>-1</sup> and growing until a confluence of 80%. Next, cells underwent serum starvation in RPMI medium with 0.05% bovine serum albumin (BSA) for 12 hours. Subsequently, the macrophages were classically activated by adding 60 ng·mL<sup>-1</sup> LPS (Sigma-Aldrich) or alternatively activated by adding 40 ng·mL<sup>-1</sup> IL-4 (PeproTech) for 12 hours before treating the cells with recombinant *Acbp* protein (100nM) for 24 hours. Data analysis was conducted by using 3 repetitions.

*Statistics* - To analyze the data, outliers were identified (ROUT method), normality was tested (Shapiro-Wilk test), followed by a two-way ANOVA, Mann-Whitney test, or a student t-test. A post hoc test was performed additionally. P-values under 0.05 were considered statistically significant. Results are displayed as mean  $\pm$  SEM. The statistical analysis was conducted using the GraphPad Prism 10 software (GraphPad Software Inc.). Additionally, the graphs were created using the same software.

HFD models ( $p = 0.0007$  for both; Figure 2e,f). A genotype effect was observed for the blood glucose, with decreased levels in the BAT-Acbp\_KO models ( $p = 0.025$ ; Figure 2d). Moreover, there tends to be a reduction in blood triglyceride levels in the BAT-Acbp-KO models (Figure 2e). In conclusion, the HFD increased *Ucp1* expression levels, body weight, blood glucose, and triglyceride levels. The BAT-Acbp-KO models showed decreased *Acbp* expression in BAT and reduced blood glucose levels.

### *Absence of ACBP in BAT induces cardiac dysfunction*

To determine the effect of ACBP on cardiac dysfunction, the heart weight tibia length (HW/TL) was measured. An enlargement of the heart was observed in the HFD groups ( $p < 0.0001$ ; Figure 3a) that tends to be higher in the BAT-Acbp-KO mice compared with the control. Considering these observations, the following cardiac remodeling genes were

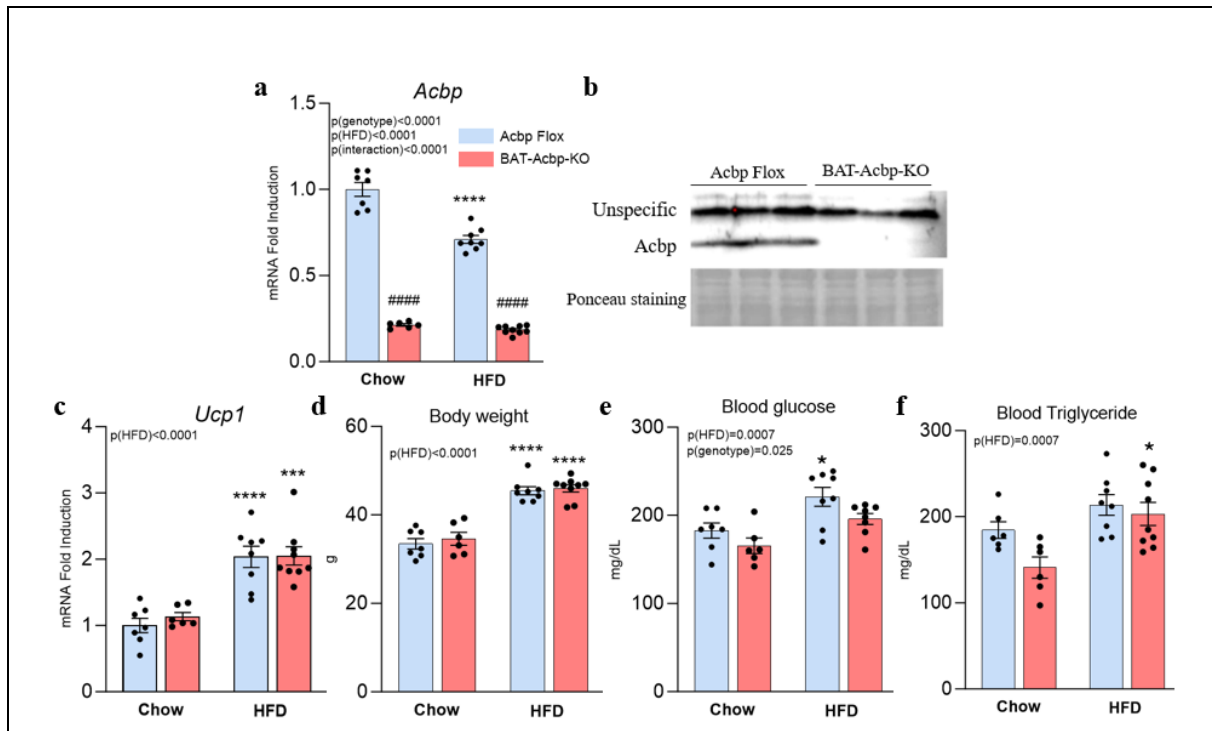


**Figure 2: Effect of *Acbp* deletion in BAT on gene expression and metabolic parameters in HFD-subjected mice.** a) Quantification of *Acbp* mRNA expression in LV. b) Protein levels of *Acbp* (1:2000) in *Acbp* Flox and BAT-*Acbp*-KO mice in BAT (n=3/group), corrected with the Ponceau staining. c) Quantification of *Ucp1* mRNA expression in LV. d) Body weight was measured in grams. e) Blood triglycerides (mg/dL). f) Blood glucose (mg/dL). All mRNA expressions and plasma metabolites were measured in *Acbp* Flox (n=7) and BAT-*Acbp*-KO (n=6) both consuming a chow diet and *Acbp* Flox (n=8) and BAT-*Acbp*-KO (n=9) both consuming an HFD. Data is presented as mean ± SEM and analyzed using a two-way ANOVA. \*p < 0.05; \*\*\*p < 0.001; \*\*\*\*p < 0.0001 for a HFD effect. #####p < 0.0001 for a genotype effect.

analyzed (atrial natriuretic factor (*Nppa*), encoding B-type natriuretic factor (*Nppb*),  $\alpha$ -myosin heavy chain (*Myh6*),  $\beta$ -myosin heavy chain (*Myh7*)) (Figure 3b-e). The BAT-*Acbp*-KO models showed increased *Nppa* in the heart (p=0.0069; Figure 3b). This effect also tends to occur for *Nppb* (Figure 3c). We also analyzed genes encoding myosin heavy chain proteins found in the sarcomere of cardiomyocytes. For the analysis of cardiac remodeling and maturity of cardiomyocytes, *Myh6* and *Myh7* were analyzed. During pathological hypertrophy, a switch from *Myh6* to *Myh7* occurs in mice, making *Myh7* more prominent (50). An elevated *Myh7* expression was observed in the BAT-*Acbp*-KO models (p=0.0077). A diet-induced effect was also observed for both *Myh6* and *Myh7* separately, decreasing the pathologic phenotype when consuming an HFD (p=0.0006). Furthermore, the ratio between the two isoforms was determined (*Myh6/Myh7*) for overall cardiac function and a decrease was found in the BAT-*Acbp*-KO models, in contrast to our control

models (p=0.0009). Besides, no dietary changes were found for the *Myh6/Myh7* ratio (Figure 3d-f). These results indicate an induction of cardiac damage in the BAT-*Acbp*-KO models.

#### *BAT-Acbp-KO* mice subjected to an HFD undergo a metabolic switch to glycolysis in the heart

The heart undergoes many metabolic changes under stress (18). Therefore, the glucose metabolism markers (pyruvate dehydrogenase inhibitor (*Pdk4*), Monocarboxylate Transporter 4 (*Mct4*), and mitochondrial pyruvate carrier 1 (*Mpc1*)) were analyzed using qPCR and western blot (Figure 4). An overall HFD effect was observed in *Pdk4* where an increase was seen for both models on protein and gene expression levels (p=0.0034; p<0.0001, respectively; Figure 4a,e). Specifically, the *Acbp* Flox model showed a significant increase in *Pdk4* on gene expression level (p=0.0373; Figure 4a). This HFD effect was also observed in the protein analysis, where a significant increase was observed in the BAT-

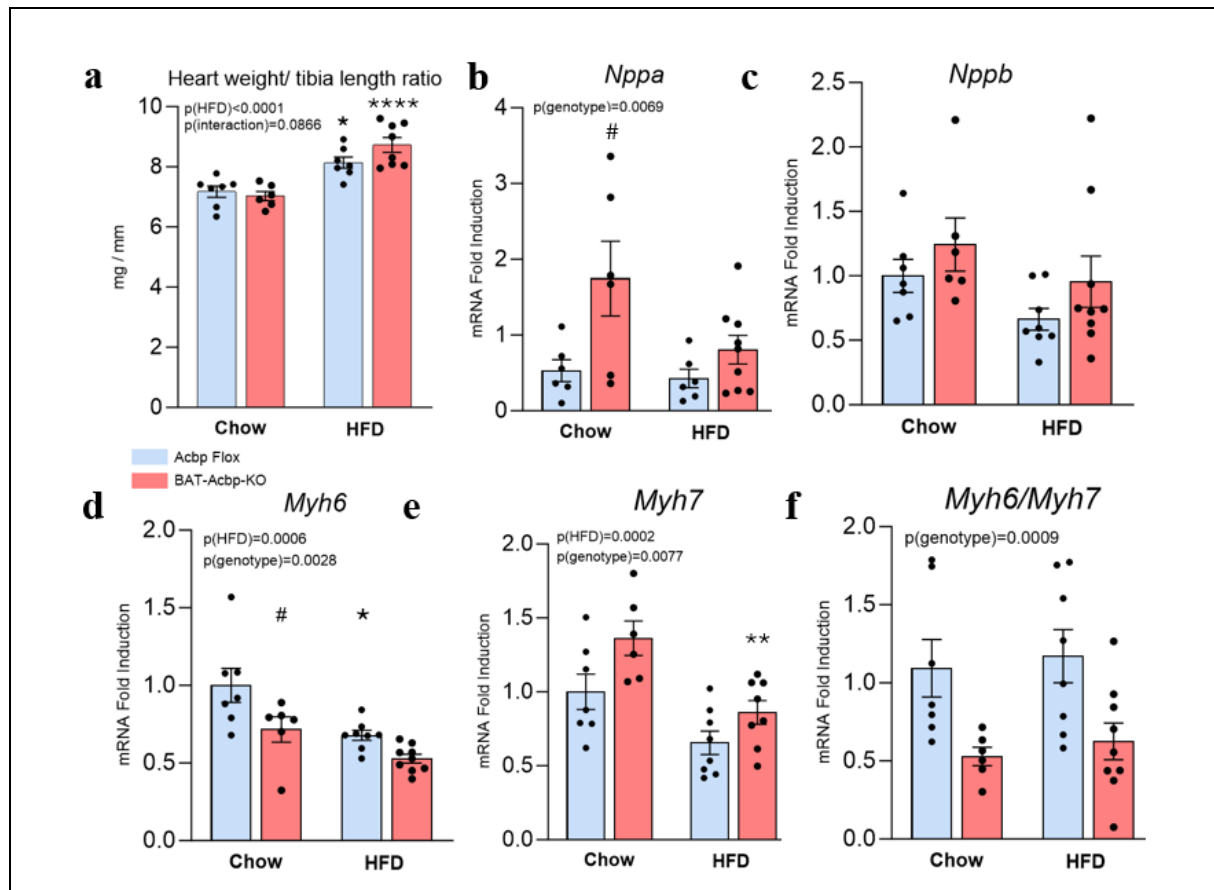


**Figure 3: Depletion of *Acbp* in BAT induces cardiac dysfunction.** a) Heart weight/tibia length ratio. mRNA gene expression of the hypertrophic markers *Nppa* (b), and *Nppb* (c) *Myh6* (d), *Myh7*(e), *Myh6/Myh7* ratio (f), in the LV of *Acbp Flox* (n=7) and *BAT-Acbp-KO* (n=6) mice both consuming a chow diet and *Acbp Flox* (n=8) and *BAT-Acbp-KO* (n=9) mice both consuming a HFD. Data is presented as mean  $\pm$  SEM and analyzed using a two-way ANOVA. \*p < 0.05; \*\*p < 0.01; \*\*\*\*p < 0.0001 for an HFD effect; #p < 0.05; for a genotype effect.

*Acbp*-KO model (p=0.0002; Figure 4d,e). On protein level, a significant increase in the lactate exporter *Mct4* was observed due to the HFD (p=0.0315), specifically in our *Acbp*-*BAT*-KO model subjected to a HFD (p=0.0204; Figure 4d,f). This also occurs with *Mpc1* protein expression, where an increase in the *BAT*-*Acbp*-KO group due to the HFD effect was found (p=0,0413; Figure 4d,g). On genotype level, all markers (*Pdk4*, *Mct4*, and *Mpc1*) showed a decrease in gene expression in the *Acbp*-*BAT*-KO models (p=0.0364; p=0.0041, p=0.0145, respectively; Figure 4a-c). The *Mct4* and *Mpc1* protein levels showed a significant interaction effect (p=0.0275; p=0.0004, respectively; Figure 4d,f,g). The protein analysis suggested a metabolic switch to glycolysis in the heart for the *BAT*-*Acbp*-Ko group subjected to an HFD. In summary, the *BAT*-*Acbp*-KO group showed increased glycolysis upon HFD.

*The BAT-Acbp-KO group showed an altered fatty acid metabolism*

Due to the high metabolic activity of the heart, some fatty acid metabolism markers (acyl-CoA dehydrogenase long chain (*Acadl*), *Acbp*, and carnitine palmitoyltransferase 1B (*Cpt1b*)) were measured using qPCR and Western blot (Figure 5). Firstly, no significant changes were found for *Acbp* in the heart (Figure 5a). On the protein level, an increase in *Cpt1b* levels was obtained in the HFD groups (p=0.0351; p=0.0005, for *Acbp Flox* and *BAT-Acbp-KO*, respectively; Figure 5d,e), while no significant differences were found for the mRNA expression of *Cpt1b* (Figure 5c). However, a general decrease of *Acadm* was seen in our *BAT*-*Acbp*-KO models (p=0.0361; Figure 5b). Overall, the *BAT*-*Acbp*-KO showed altered fatty acid metabolism upon HFD.

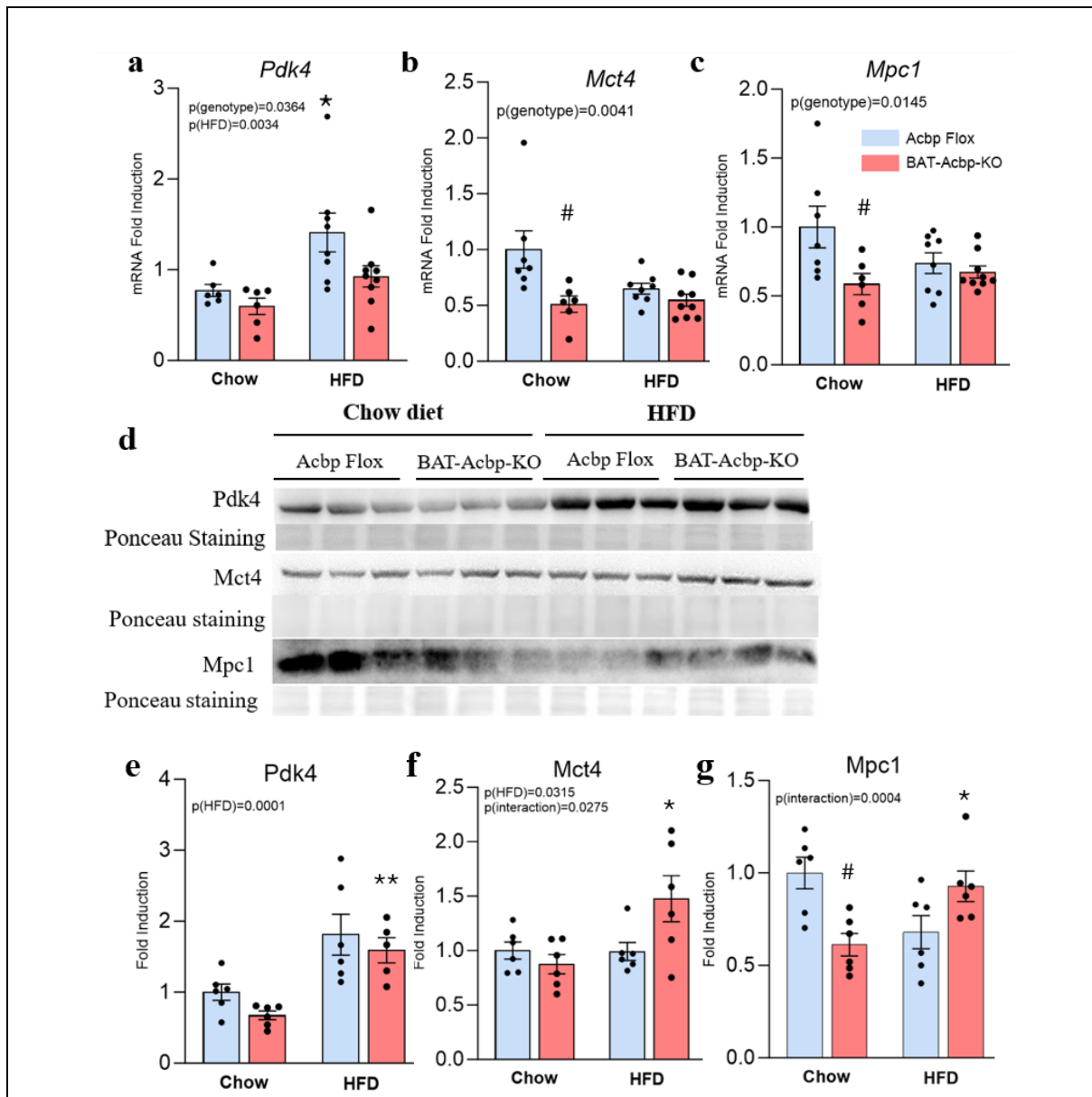


**Figure 4: BAT-Acbp-KO alters cardiac glycolytic markers upon HFD.** mRNA expression in the heart using metabolic markers Pdk4 (a), Mct4 (b), and Mpc1 (c) in Acbp Flox (n=7) and BAT-Acbp-KO (n=6) both consuming a chow diet and Acbp Flox (n=8) and BAT-Acbp-KO (n=9) both consuming a HFD. **d** Western blot analysis of the heart tissue using the following proteins Pdk4, Mct4, and Mpc1. Quantification of the western blot analysis of Pdk4 (1:5000) (e), Mct4 (1:1000) (f), and Mpc1 (1:1000) (g) (n=6/group) normalized using the Ponceau Staining. Data is presented as mean ± SEM and analyzed using a two-way ANOVA. \*p < 0.05; \*\*p < 0.01 for a HFD effect. #p < 0.05 for a genotype effect.

*A lack of Acbp in BAT reduces HFD-induced fibrosis*

For the analysis of cardiac fibrosis, the following fibrotic genes were measured (Collagen type III alpha I (*Col3a1*), Collagen type I alpha I (*Col1a1*), Matrix metalloproteinase 9 (*Mmp9*), and TIMP Metalloproteinase Inhibitor 1 (*Timp1*); Figure 6). For the HFD effect, an overall significant increase was observed in *Col3a1* (p<0.0001), and a specific increase was

analyzed for the BAT-Acbp-KO model (p=0.0017; Figure 6a). On the contrary, an overall decrease in fibrosis was observed for the *Mmp9/Timp1* ratio in the HFD groups (p=0.0002; Figure 6e). A reduction in *Mmp9* expression was measured upon HFD, specifically in the BAT-Acbp-KO group (p=0.0008; p=0.0013, respectively; Figure 6c). Consistently with the increased *Timp1* expression upon HFD,

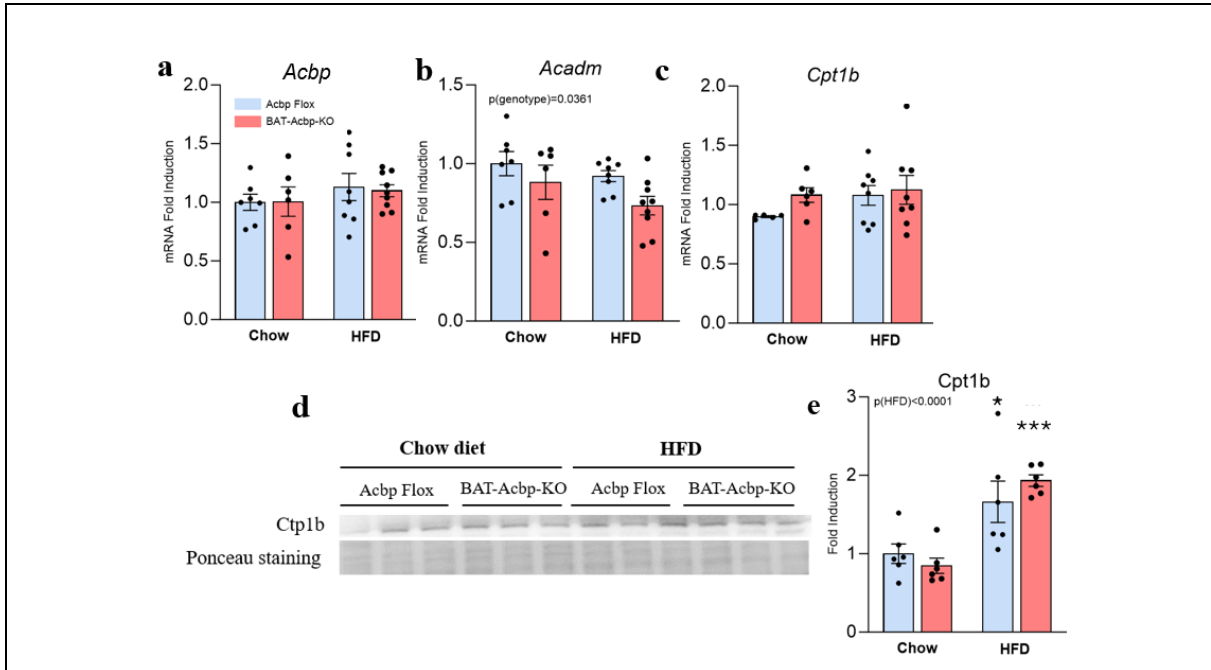


**Figure 5: ACBP alters fatty acid metabolism markers upon HFD.** mRNA expression in the heart using metabolic markers *Acbp* (a), *Acadm* (b), and *Cpt1b* (c) in *Acbp Flox* (n=7) and *BAT-Acbp-KO* (n=6) both consuming a chow diet and *Acbp Flox* (n=8) and *BAT-Acbp-KO* (n=9) both consuming an HFD. **d**) Western blot analysis of *Cpt1b* (1:1000) in the heart tissue. **e**) Quantification of the *Cpt1b* western blot analysis (n=6/group). Data is presented as mean ± SEM and analyzed using a two-way ANOVA. \*p < 0.05; \*\*\*p < 0.001; for a HFD effect.

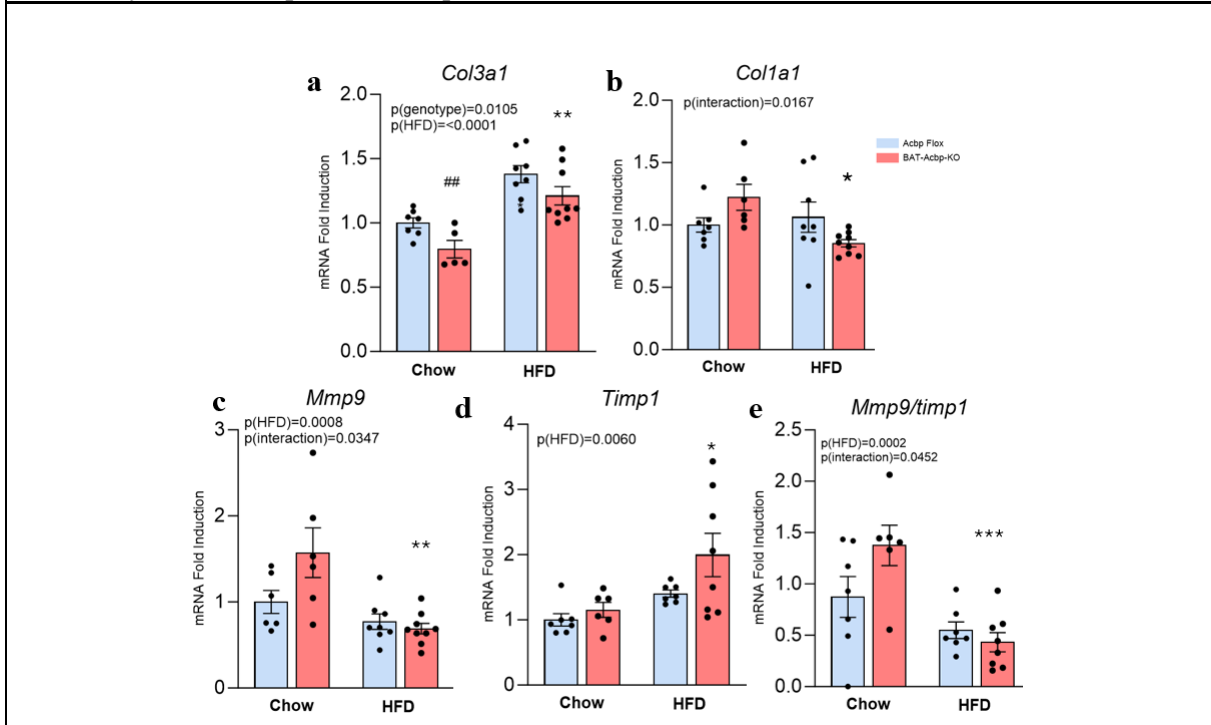


**Figure 6: Absence of ACBP in BAT reduces fibrosis in heart tissue.** mRNA expression of fibrotic genes *Col3A1* (a), *Col1A1* (b), *Mmp9* (c), *Timp1* (d) and the *Mmp9/Timp1* ratio (e) in LV of *Acbp Flox* (n=7) and *BAT-Acbp-KO* (n=6) mice both consuming a chow diet and *Acbp Flox* (n=8) and *BAT-Acbp-KO* (n=9) mice both consuming an HFD. Data is presented as mean ± SEM and analyzed using a two-way ANOVA. \*p < 0.05; \*\*p < 0.01; \*\*\*p < 0.001 for an HFD effect; ##p < 0.01; for a genotype effect.

specifically in the BAT-Acbp-KO group ( $p=0.0060$ ;  $p=0.0494$ , respectively; Figure 6d). Moreover, a significant decrease of *Coll1a1* was observed in the Acbp- BAT-KO model subjected to an HFD ( $p=0.0301$ ; Figure 6b). As for the genotype effect, a significant reduction in *Col3a1* expression was observed in our BAT-Acbp-KO models ( $p=0.0105$ ; Figure 6a). Lastly, an overall significant interaction effect was observed for the *Coll1A1*, *Mmp9*, and the *Mmp9/Timp1* ratio ( $p=0.0167$ ;  $p=0.0347$ ;  $p=0.0452$ , respectively; Figure 6b,c,e). These results indicate that the BAT-Acbp-KO group is protected against fibrosis upon HFD.

*ACBP alters macrophage polarization and inflammation*

Since macrophages are the first immune cells to invade cardiac tissue and initiate fibrotic pathways, it seemed interesting to analyze the

effect of Acbp independently on the macrophage M1 and M2 phenotypes (16). The RAW264.7 cell culture was treated with recombinant Acbp and qPCR measurements were performed. Acbp induced increased expression of M1 phenotype markers Nitric oxide synthase (*Nos2*), Tumor necrosis factor (*Tnfa*), and C-C Motif Chemokine Ligand 2 (*Ccl2*) in monocytes ( $p=0.001$ ;  $p<0.0001$ ;  $p<0.0001$ , respectively; Figure 7a-c). This effect also occurred in the M2 phenotype ( $p=0.001$ ;  $p=0.0004$ ;  $p=0.0002$ , respectively; Figure 7a-c). The mRNA expression of the M2 marker *Mrc1* was unaltered upon ACBP treatment (Figure 7d). The M2 marker *Arg1* showed an increased expression in the M2 group when treated with Acbp ( $p<0.0001$ ; Figure 7e). Overall, Acbp induces a pro-inflammatory M1 phenotype in macrophages.

The heart tissue of the BAT-Acbp-KO and Acbp Flox groups upon chow or HFD diet

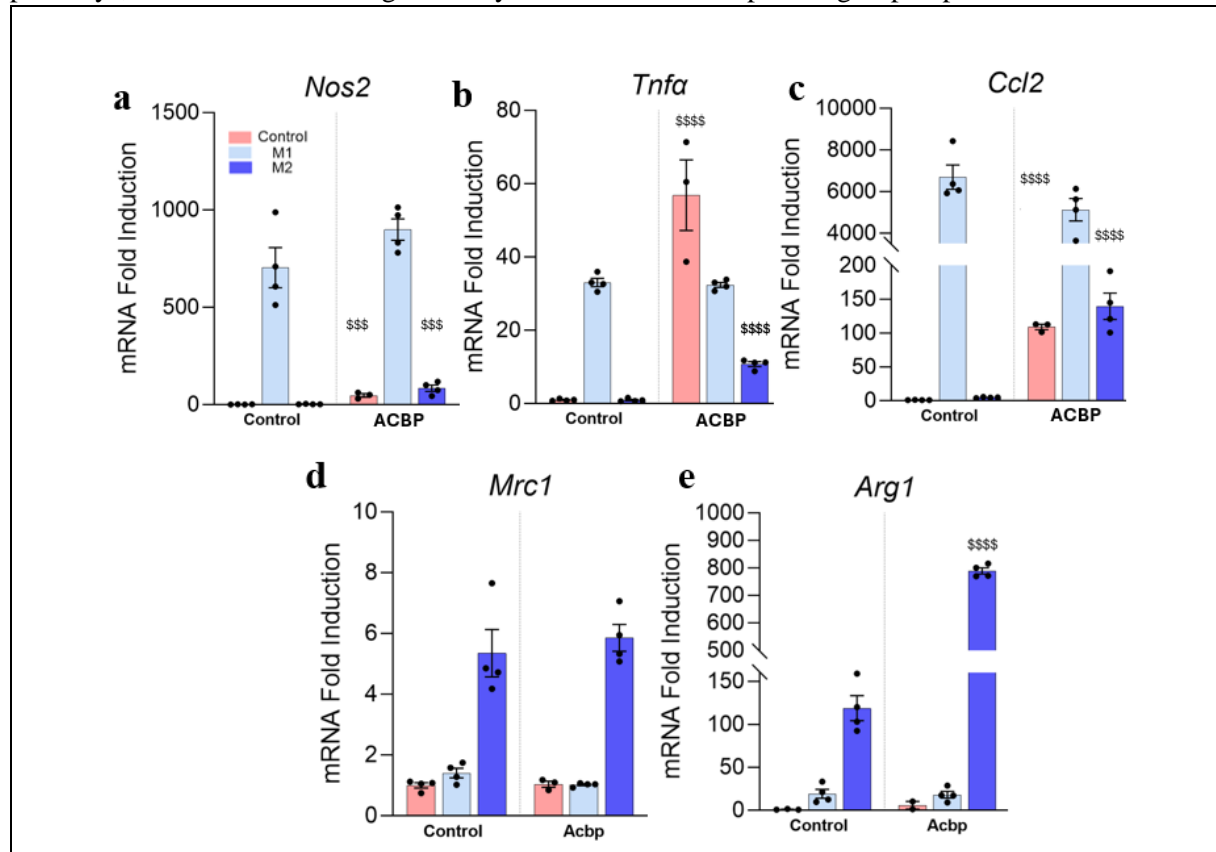


**Figure 7: ACBP promotes a pro-inflammatory phenotype (M1) in macrophages *in vitro*.** Macrophages (control (red), M1 (light blue), and M2 (dark blue)) were treated with recombinant Acbp protein (100nM) for 24 hours after pre-treatment with LPS (60ng/ml) or IL-4 (40ng/ml) for stimulation of M1 or M2 phenotype, respectively. mRNA expression was measured for M1 macrophage phenotype markers *Nos2* (a), *Tnfa* (b), and *Ccl2*(c) ( $n=4$ /all groups except for control ACBP group ( $n=3$ )). mRNA expression levels of M2 macrophage phenotype markers *Mrc1* (d) and *Arg1* (e) ( $n=4$ /all groups except for control ACBP group ( $n=3$ )). Data is presented as mean  $\pm$  SEM and analyzed using a multiple unpaired student t-test and two-way ANOVA. \$\$\$ $p < 0.001$ ; \$\$\$\$ $p < 0.0001$  for an ACBP effect.

was analyzed using qPCR, where we measured inflammatory markers Interleukin 1 Beta (*Il1b*) and *Tnf*. An overall HFD effect was observed for the *Il1b* expression, reducing inflammation in the HFD groups ( $p=0.0020$ ; Figure 8a). An interaction effect was discovered for the *Tnf* expression between the BAT-Acbp-KO group ( $p=0.0110$ ; Figure 8b). Specifically, a decreased *Il1b* and *Tnf* expression was observed for the BAT-Acbp-KO group due to the HFD ( $p=0.0162$ ;  $p=0.0245$ , respectively; Figure 8a,b). The *Tnf* expression even tends to be lower in the BAT-Acbp-KO group compared with the Acbp Flox both subjected to an HFD. Additionally, we found an overall diet-induced decrease in the *Mrc1* expression ( $p=0.0002$ ), specifically in the BAT-Acbp-KO group ( $p=0.003$ ; Figure 8c). The *Arg1* group seemed to show consistent results, reducing anti-inflammatory markers upon HFD in the Bat-Acbp-KO group (Figure 8d). Deletion of *Acbp* in BAT altered inflammatory markers in the heart.

## DISCUSSION

This study identified ACBP as a factor involved in myocardium remodeling upon HFD-induced obesity. Preliminary data from our laboratory showed that BAT is the most prominent organ to express *Acbp*. Therefore, it seemed interesting to perform a BAT-Acbp-KO and investigate the myocardium. Besides this, researchers have found several factors secreted by BAT to influence cardiac function. For example, BAT-secreted proteins Fgf21 and Il-6 protect the heart against cardiac hypertrophy and inflammatory effects respectively (58, 59). The association between the BAT and the heart is also metabolic, indicating that an active BAT decreases the prevalence of obesity which is a risk factor for CVD by burning glucose and triglycerides (39). Overall, we observed increased cardiac dysfunction/pathological

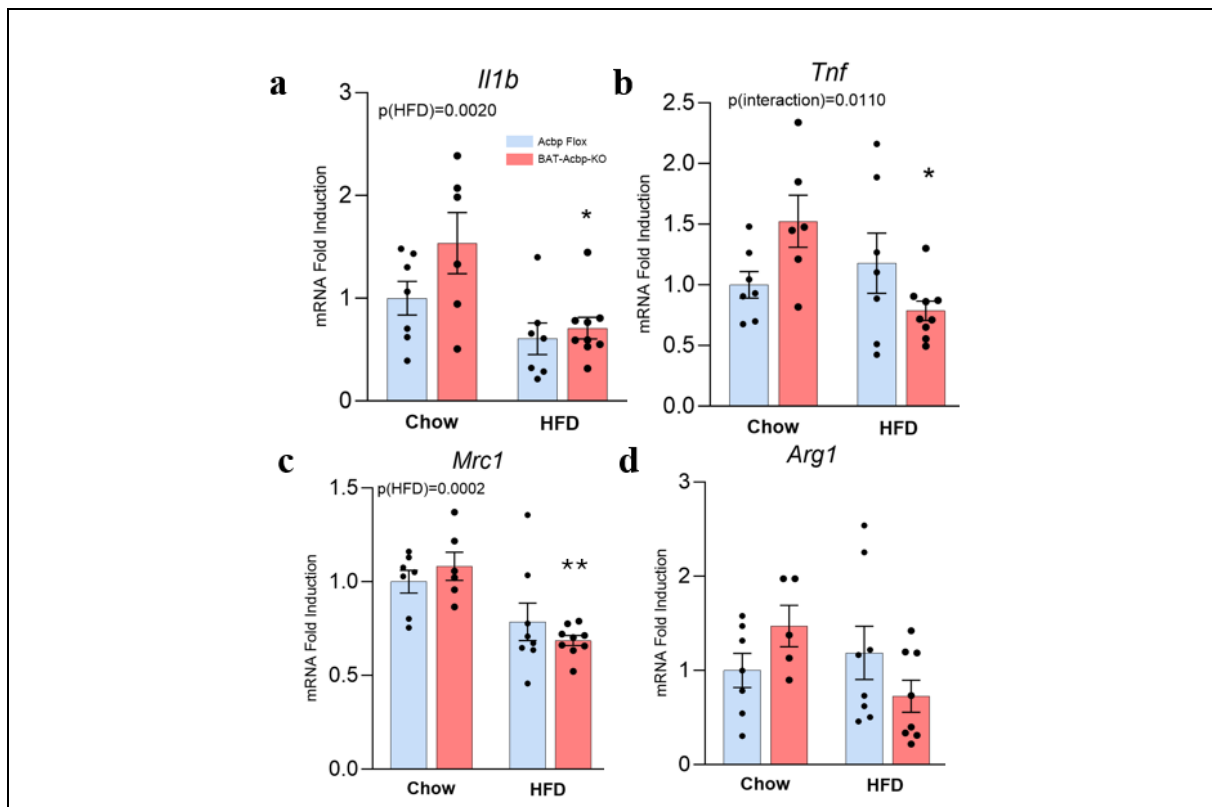


**Figure 8: Deletion of ACBP in BAT alters inflammatory phenotype in the heart.** Macrophages (control (red), M1 (light blue), and M2 (dark blue)) were treated with recombinant *Acbp* protein (100nM) for 24 hours after pre-treatment with LPS (60ng/ml) or IL-4 (40ng/ml) for stimulation of M1 or M2 phenotype, respectively. mRNA expression levels of anti-inflammatory markers *Mrc1*(c) and *Arg1*(d) in heart tissue of *Acbp Flox* (n=7) and *BAT-Acbp-KO* (n=6) both consuming a chow diet and *Acbp Flox* (n=8) and *BAT-Acbp-KO* (n=9) both consuming an HFD. Data is presented as mean  $\pm$  SEM and analyzed using a multiple unpaired student t-test and two-way ANOVA. \* $p < 0.05$ ; \*\* $p < 0.01$  for an HFD effect.

hypertrophy markers, reduced fibrosis, and changes in metabolism markers in our specific BAT-Acbp-KO model upon HFD.

The *Acbp* gene expression was first measured in the BAT-Acbp-KO model to confirm the KO. Due to the dynamic interplay between cells in the BAT (including macrophages, sympathetic neurons, immune cells, and others) a residual *Acbp* expression could be measured as RNA in BAT-Acbp-KO by qPCR. (60, 61). Also, *Ucp1* was overexpressed in BAT with HFD for both genotypes. This is a typical feature of diet-induced obesity as previously reported (57, 62). Furthermore, *Ucp1* was inversely correlated to *Acbp* expression in *Acbp* Flox mice, a finding we have described in other different wild-type mice models (unpublished).

In the HFD groups, a significant increase in body weight and HW/TL was measured due to the increase in fat intake (63, 64). Triggers such as an HFD can induce pathological hypertrophy due to increased blood pressure or volume overload, which is associated with contractility impairment and altered pumping functioning of the heart (65, 66). In this study, we saw a tendency in our BAT-Acbp-KO group subjected to an HFD to have an increased HW/TL ratio compared with the *Acbp* Flox group upon HFD. We were therefore interested in the gene expression levels of genes usually associated with cardiac dysfunction and hypertrophy. Supported by other studies, pathologic cardiac hypertrophy is associated with a switch to fetal genes, resulting in upregulation of the *Myh7* rather than *Myh6*, the same pattern of expression that we described for the BAT-Acbp-KO mice (67, 68). This upregulation of fetal genes suggests decreased cardiomyocyte contractility and therefore increased myocardial stiffness (67). Our results showed a reduction in *Myh6* and 7 gene expressions in the HFD models. This is opposite to previous studies where HFD-subjected mice showed increased hypertrophy in the heart and increased expression of *Myh7* rather than *Myh6* (69, 70). A possible explanation can be that C57/B16 mice are resistant to HFD effects or the duration of the HFD. *Nppa* (Anp) and *Nppb* (Bnp) are upregulated in a hypertrophic heart and secreted upon increased wall stretch (71). Consistently with our results, a more prominent expression of *Nppa* rather than *Nppb* was

measured in the BAT-Acbp-KO groups. Upon HFD, no significant differences were found, but researchers have found that *Nppa* and *Nppb* gene expression was reduced in cardiac tissue of obese rats (72). Accordingly, the natriuretic peptides showed low plasma levels in people with obesity, which could be due to a reduced secretion of natriuretic peptides from the heart (73, 74).

As mentioned before, the heart undergoes a switch to a fetal metabolic profile in cardiac hypertrophy, increasing glycolysis and decreasing fatty acid metabolism (75). In an acute way, the switch to glycolysis is beneficial for the maintenance of cardiac function in basal conditions. However, in the long-term, this change in metabolism is not beneficial to meet the energetic demands of the heart, since it can be not only the consequence but also the cause of cardiac hypertrophy and dysfunction (76, 77).

In our study, increased protein and gene expression levels of *Pdk4* were found in the HFD groups, indicating an increased fatty acid metabolism in the heart (78, 79). It is known that animals subjected to a long-term HFD induce cardiac *Pdk4* expression, confirming our HFD models which were subjected to an HFD for 12 weeks (80). However, the *Pdk4* protein levels showed this increase to a lesser extent in the BAT-Acbp-KO groups compared with the *Acbp* flox groups. The absence of ACBP in BAT could influence energy substrate availability for the heart and induce this switch to glycolysis (81).

In pathological conditions, the heart also increases lactate transport to improve cardiac functions (82). In our study, we described an increase in lactate exporter *Mct4* protein levels upon HFD, specifically in our BAT-Acbp-KO group. Consistently, researchers have found upregulated *Mct4* to induce cardiac hypertrophy due to altered energy demand and substrate availability and also in leptin receptor-deficient mice (83, 84). Moreover, elevated plasma levels of lactate were observed in people with obesity, indicating an increased lactate efflux mediated by MCT4 (85, 86). On the contrary, the gene expression levels of *Mct4* showed an overall significant decrease in our BAT-Acbp-KO group. A significant decrease of *Mpc1* protein expression in the BAT-Acbp-KO was observed compared with the *Acbp* Flox upon chow diet. In contrast to our results, *Mpc1* expression was

downregulated in hypertrophic hearts of humans and mice due to the switch to glycolysis in this condition (87). *Mpc1* gene expression showed a significant difference between the 2 genotypes. This difference between gene and protein expression might be due to post-translational or -transcriptional modifications. Increased protein levels of *Mpc1* in the BAT-Acbp-KO group upon HFD could also be a reflection of the impaired cardiac metabolic status of these mice. In cardiac hypertrophy, impaired mitochondrial pyruvate uptake leads to reliance on glycolysis (87). However, during increased metabolic demand in HFD conditions, the heart may upregulate mitochondrial components, such as *Mpc1* (88). In obese mice with a C57BL/6 background, no significant differences were found in the expression of *Mpc1* compared with WT (89). *Mpc1*<sup>-/-</sup> mice even improved heart failure upon HFD (90). It is still unknown how the *Mpc1* expression is altered upon HFD.

The fatty acid metabolism marker *Acadm* (*Mcad*) showed a significant reduction in the BAT-Acbp-KO mice, indicating reduced FA utilization and increased glycolysis (88). The protein expression of *Cpt1b*, another FA metabolism marker and the central point of  $\beta$ -oxidation regulation (91), showed increased levels upon HFD, specifically in the BAT-Acbp-KO group. In HFD, increased availability of FFA causes increased FA metabolism (92). The deletion of ACBP in BAT disrupted lipid metabolism in BAT and might have an overall effect on metabolic homeostasis, including the heart (39). The metabolic markers show that our BAT-Acbp-KO model increased the metabolic demand and uses different substrates to maintain cardiac function (88). Glycemia and triglyceride levels were decreased in both BAT-Acbp-KO models, suggesting a potential circulating metabolite clearance by the heart.

The ECM of the heart consists of *Colla1* (85%) and *Col3a1* (11%) secreted by CF (7, 11). Obesity is strongly associated with cardiac fibrosis which is related to metabolic dysfunction, insulin resistance, and hyperglycemia, however, the exact mechanisms remain poorly understood (5). Researchers have found an induction of cardiac fibrosis in HFD models (93, 94). The diet-induced obesity model used in this study has more subtle effects on the

myocardium. Diet-induced cardiac fibrosis has been described in an HFD model of a minimum of 6-8 months in C57BL/6 mice with increased collagen expression (95, 96). A significant increase of *Col3a1* was observed upon HFD, specifically in our BAT-Acbp-KO model. Increased levels of *Col3a1* cause cardiac fibrosis (97). For the *Colla1* expression, a decrease between our BAT-Acbp-KO groups was found upon HFD, indicating protection against fibrosis (97). Additionally, in the BAT-Acbp-KO groups, a significant decrease in *Col3a1* was measured, specifying a protective genotypical effect (97). *Mmp9* degrades the ECM, while *Timp1* inhibits this process (98). An imbalance of these two factors initiates several pathologies, including cardiac fibrosis and inflammation. In this study, a decrease in *Mmp9* expression was observed in the HFD groups, specifically the BAT-Acbp-KO group, which is associated with protection against fibrosis (99). These findings are confirmed by the upregulation of *Timp1* in the HFD groups (98).

Cardiac fibrosis and inflammation show a very strong association. Consistently with our fibrosis and *in vitro* results, the inflammatory cytokines *Il1 $\beta$*  and *Tnf* were decreased in the BAT-Acbp-KO group upon HFD. This suggests that depletion of ACBP in BAT modulates the inflammatory response associated with obesity. The inflammatory response induced by obesity can be influenced by lipid overload (18). In case of cardiac injury, M1 macrophages are recruited to the site of injury and activate fibroblasts for the production of ECM (19). ACBP increased the M1 phenotype in a macrophage cell culture. (33).

The induction of hypertrophy in the BAT-Acbp-KO groups suggests that deletion of ACBP induced cardiac stress and dysfunction. As ACBP influences beta-oxidation and BAT relies on this for proper thermogenesis, deletion of ACBP in BAT could impair energy balance in the heart (41, 88). Despite the cardiac dysfunction analyzed in this model, a reduction of fibrosis and inflammation was observed in this model upon HFD, proposing an activation of anti-inflammatory and anti-fibrotic pathways. Deletion of ACBP could alter the BAT signaling molecules (batokines) and induce anti-fibrotic or anti-inflammatory effects. Another reason can be an enhanced lipid handling by the heart causing a

decrease in lipid overload and pro-inflammatory markers. The natriuretic peptides are upregulated upon cardiac hypertrophy but exert inhibitory effects on cardiac fibroblasts (100).

The cardiac phenotype obtained in our BAT-Acbp-KO model upon HFD gained our interest in the underlying mechanisms. ACBP levels are upregulated in obesity and CVD (24, 28, 33), removal of ACBP from BAT could thereby alter ACBP circulating levels and exert obesity-induced cardiac effects. Another plausible mechanism in our BAT-Acbp-KO is a potential change in BAT secretome due to the deletion of ACBP. Signaling molecules (batokines) secreted by BAT can influence other peripheral organs, including the heart (101). As mentioned earlier, changes in batokine levels such as Il-6 and FGF21 could induce cardiac remodeling and alter cardiac function (58, 59). Deletion of ACBP in the BAT, which is a metabolic active organ and contributes to lipid metabolism and energy expenditure (53, 102), could influence the cardiac changes observed. This BAT-Acbp-KO might have disrupted lipid metabolism and thermogenesis, thereby inducing metabolic stress. Fatty acid oxidation is the primary source of energy for the heart, which is highly metabolically active (103). Due to this metabolic disturbance in the BAT, the heart needs to adapt and this could lead to the cardiac dysfunction observed in this study (88).

Future implications in the involvement of ACBP secreted by BAT on CVD include investigation in other obesity models, including genetic models to obtain more information about the diet-induced effect of ACBP. Moreover, other typical cardiac dysfunction models (doxorubicin, isoproterenol, and genetic models) could be used to examine the ACBP model on CVD. Studies applied in female mice could result in different results due to hormonal changes and different fat distribution. Analyzing circulating ACBP levels could give us an indication of a direct or indirect effect on the heart in our BAT-Acbp-KO model. Moreover, identifying the specific batokines and functional pathways in the BAT-Acbp-KO model could be interesting in examining the association between ACBP, BAT, and cardiac effects. Lastly, chronic exposure to HFD and the association with ACBP, BAT, and CVD could be interesting

to analyze due to the different effects observed in previous studies.

## CONCLUSION

In conclusion, this research provides insights into the cardiac effects obtained in a BAT-Acbp-KO model upon HFD. The findings suggest an increase in cardiac dysfunction, reduced cardiac fibrosis, increased glycolytic markers, altered fatty acid markers, and decreased inflammation. The involvement of ACBP in numerous metabolic pathways and myocardial remodeling suggests its influence on CVD pathologies. Therefore, targeting ACBP and its pathways can be promising for mitigating the burden of CVD. Further research needs to be performed to unravel the exact mechanisms of ACBP in BAT and CVD.

## REFERENCE

1. Robinson WF, Robinson NA. Chapter 1 - Cardiovascular System. In: Maxie MG, editor. Jubb, Kennedy & Palmer's Pathology of Domestic Animals: Volume 3 (Sixth Edition): W.B. Saunders; 2016. p. 1-101.e1.
2. Cardiovascular diseases World health organisation 2024 [Available from: [https://www.who.int/health-topics/cardiovascular-diseases#tab=tab\\_1](https://www.who.int/health-topics/cardiovascular-diseases#tab=tab_1)].
3. Teo KK, Rafiq T. Cardiovascular Risk Factors and Prevention: A Perspective From Developing Countries. *Can J Cardiol*. 2021;37(5):733-43.
4. Powell-Wiley TM, Poirier P, Burke LE, Després JP, Gordon-Larsen P, Lavie CJ, et al. Obesity and Cardiovascular Disease: A Scientific Statement From the American Heart Association. *Circulation*. 2021;143(21):e984-e1010.
5. Cavalera M, Wang J, Frangogiannis NG. Obesity, metabolic dysfunction, and cardiac fibrosis: pathophysiological pathways, molecular mechanisms, and therapeutic opportunities. *Transl Res*. 2014;164(4):323-35.
6. Frangogiannis NG. Cardiac fibrosis. *Cardiovasc Res*. 2021;117(6):1450-88.
7. Maruyama K, Imanaka-Yoshida K. The Pathogenesis of Cardiac Fibrosis: A Review of Recent Progress. *Int J Mol Sci*. 2022;23(5).
8. Liu M, López de Juan Abad B, Cheng K. Cardiac fibrosis: Myofibroblast-mediated pathological regulation and drug delivery strategies. *Adv Drug Deliv Rev*. 2021;173:504-19.
9. Lo CS, Chen ZH, Hsieh TJ, Shin SJ. Atrial natriuretic peptide attenuates high glucose-activated transforming growth factor-beta, Smad and collagen synthesis in renal proximal tubular cells. *J Cell Biochem*. 2008;103(6):1999-2009.
10. Tschöpe C, Lam CSP. Diastolic heart failure: What we still don't know. *Herz*. 2012;37(8):875-9.
11. Hinderer S, Schenke-Layland K. Cardiac fibrosis – A short review of causes and therapeutic strategies. *Advanced Drug Delivery Reviews*. 2019;146:77-82.
12. Gallo S, Vitacolonna A, Bonzano A, Comoglio P, Crepaldi T. ERK: A Key Player in the Pathophysiology of Cardiac Hypertrophy. *Int J Mol Sci*. 2019;20(9).
13. Nakamura M, Sadoshima J. Mechanisms of physiological and pathological cardiac hypertrophy. *Nature Reviews Cardiology*. 2018;15(7):387-407.
14. Frey N, Olson EN. Modulating Cardiac Hypertrophy by Manipulating Myocardial Lipid Metabolism? *Circulation*. 2002;105(10):1152-4.
15. Ren J, Wu NN, Wang S, Sowers JR, Zhang Y. Obesity cardiomyopathy: evidence, mechanisms, and therapeutic implications. *Physiological Reviews*. 2021;101(4):1745-807.
16. Mouton AJ, Li X, Hall ME, Hall JE. Obesity, Hypertension, and Cardiac Dysfunction: Novel Roles of Immunometabolism in Macrophage Activation and Inflammation. *Circ Res*. 2020;126(6):789-806.
17. DeBerge M, Shah SJ, Wilsbacher L, Thorp EB. Macrophages in Heart Failure with Reduced versus Preserved Ejection Fraction. *Trends Mol Med*. 2019;25(4):328-40.
18. Lafuse WP, Wozniak DJ, Rajaram MVS. Role of Cardiac Macrophages on Cardiac Inflammation, Fibrosis and Tissue Repair. *Cells*. 2020;10(1).
19. Ploeger DT, Hosper NA, Schipper M, Koerts JA, de Rond S, Bank RA. Cell plasticity in wound healing: paracrine factors of M1/ M2 polarized macrophages influence the phenotypical state of dermal fibroblasts. *Cell Commun Signal*. 2013;11(1):29.
20. Cucchi D, Camacho-Muñoz D, Certo M, Pucino V, Nicolaou A, Mauro C. Fatty acids - from energy substrates to key regulators of cell survival, proliferation and effector function. *Cell Stress*. 2019;4(1):9-23.
21. Yeh TL, Chen HH, Tsai SY, Lin CY, Liu SJ, Chien KL. The Relationship between Metabolically Healthy Obesity and the Risk of Cardiovascular Disease: A Systematic Review and Meta-Analysis. *J Clin Med*. 2019;8(8).

22. Murashige D, Jang C, Neinast M, Edwards JJ, Cowan A, Hyman MC, et al. Comprehensive quantification of fuel use by the failing and nonfailing human heart. *Science*. 2020;370(6514):364-8.
23. van der Vusse GJ, van Bilsen M, Glatz JFC. Cardiac fatty acid uptake and transport in health and disease. *Cardiovascular Research*. 2000;45(2):279-93.
24. Montégut L, Joseph A, Chen H, Abdellatif M, Ruckenstein C, Motiño O, et al. High plasma concentrations of acyl-coenzyme A binding protein (ACBP) predispose to cardiovascular disease: Evidence for a phylogenetically conserved proaging function of ACBP. *Aging Cell*. 2023;22(1):e13751.
25. Motiño O, Lambertucci F, Anagnostopoulos G, Li S, Nah J, Castoldi F, et al. ACBP/DBI protein neutralization confers autophagy-dependent organ protection through inhibition of cell loss, inflammation, and fibrosis. *Proc Natl Acad Sci U S A*. 2022;119(41):e2207344119.
26. Charmpilas N, Ruckenstein C, Sica V, Büttner S, Habernig L, Dichtinger S, et al. Acyl-CoA-binding protein (ACBP): a phylogenetically conserved appetite stimulator. *Cell Death Dis*. 2020;11(1):7.
27. Montégut L, Abdellatif M, Motiño O, Madeo F, Martins I, Quesada V, et al. Acyl coenzyme A binding protein (ACBP): An aging- and disease-relevant "autophagy checkpoint". *Aging Cell*. 2023;22(9):e13910.
28. Li S, Joseph A, Martins I, Kroemer G. Elevated plasma levels of the appetite-stimulator ACBP/DBI in fasting and obese subjects. *Cell Stress*. 2021;5(7):89-98.
29. Bravo-San Pedro JM, Sica V, Martins I, Anagnostopoulos G, Maiuri C, Kroemer G. Cell-autonomous, paracrine and neuroendocrine feedback regulation of autophagy by DBI/ACBP (diazepam binding inhibitor, acyl-CoA binding protein): the obesity factor. *Autophagy*. 2019;15(11):2036-8.
30. Alquier T, Christian-Hinman CA, Alfonso J, Færgeman NJ. From benzodiazepines to fatty acids and beyond: revisiting the role of ACBP/DBI. *Trends Endocrinol Metab*. 2021;32(11):890-903.
31. Klionsky DJ, Petroni G, Amaravadi RK, Baehrecke EH, Ballabio A, Boya P, et al. Autophagy in major human diseases. *Embo j*. 2021;40(19):e108863.
32. Joseph A, Chen H, Anagnostopoulos G, Montégut L, Lafarge A, Motiño O, et al. Effects of acyl-coenzyme A binding protein (ACBP)/diazepam-binding inhibitor (DBI) on body mass index. *Cell Death Dis*. 2021;12(6):599.
33. Bravo-San Pedro JM, Sica V, Martins I, Pol J, Loos F, Maiuri MC, et al. Acyl-CoA-Binding Protein Is a Lipogenic Factor that Triggers Food Intake and Obesity. *Cell Metab*. 2019;30(4):754-67.e9.
34. Jacob JB, Wei KC, Bepler G, Reyes JD, Cani A, Polin L, et al. Identification of actionable targets for breast cancer intervention using a diversity outbred mouse model. *iScience*. 2023;26(4):106320.
35. Atak A, Khurana S, Gollapalli K, Reddy PJ, Levy R, Ben-Salmon S, et al. Quantitative mass spectrometry analysis reveals a panel of nine proteins as diagnostic markers for colon adenocarcinomas. *Oncotarget*. 2018;9(17):13530-44.
36. Harris FT, Rahman SM, Hassanein M, Qian J, Hoeksema MD, Chen H, et al. Acyl-coenzyme A-binding protein regulates Beta-oxidation required for growth and survival of non-small cell lung cancer. *Cancer Prev Res (Phila)*. 2014;7(7):748-57.
37. Duman C, Yaqubi K, Hoffmann A, Acikgöz AA, Korshunov A, Bendszus M, et al. Acyl-CoA-Binding Protein Drives Glioblastoma Tumorigenesis by Sustaining Fatty Acid Oxidation. *Cell Metab*. 2019;30(2):274-89.e5.
38. Yao J, Liu Y, Yang J, Li M, Li S, Zhang B, et al. Single-Cell Sequencing Reveals that DBI is the Key Gene and Potential Therapeutic Target in Quiescent Bladder Cancer Stem Cells. *Front Genet*. 2022;13:904536.
39. Chen HJ, Meng T, Gao PJ, Ruan CC. The Role of Brown Adipose Tissue Dysfunction in the Development of Cardiovascular Disease. *Front Endocrinol (Lausanne)*. 2021;12:652246.
40. Marlatt KL, Ravussin E. Brown Adipose Tissue: an Update on Recent Findings. *Curr Obes Rep*. 2017;6(4):389-96.
41. Garside JC, Livingston EW, Frank JE, Yuan H, Branca RT. In vivo imaging of brown adipose tissue vasculature reactivity during adrenergic stimulation of non-shivering thermogenesis in mice. *Scientific Reports*. 2022;12(1):21383.

42. Maliszewska K, Kretowski A. Brown Adipose Tissue and Its Role in Insulin and Glucose Homeostasis. *Int J Mol Sci.* 2021;22(4).
43. Lee J, Ellis JM, Wolfgang MJ. Adipose fatty acid oxidation is required for thermogenesis and potentiates oxidative stress-induced inflammation. *Cell Rep.* 2015;10(2):266-79.
44. Villarroya F, Cereijo R, Villarroya J, Giralt M. Brown adipose tissue as a secretory organ. *Nature Reviews Endocrinology.* 2017;13(1):26-35.
45. Liu X, Wang S, You Y, Meng M, Zheng Z, Dong M, et al. Brown Adipose Tissue Transplantation Reverses Obesity in Ob/Ob Mice. *Endocrinology.* 2015;156(7):2461-9.
46. Saito M, Okamatsu-Ogura Y, Matsushita M, Watanabe K, Yoneshiro T, Nio-Kobayashi J, et al. High incidence of metabolically active brown adipose tissue in healthy adult humans: effects of cold exposure and adiposity. *Diabetes.* 2009;58(7):1526-31.
47. Bhuiyan J, Pritchard PH, Pande SV, Seccombe DW. Effects of high-fat diet and fasting on levels of acyl-coenzyme A binding protein in liver, kidney, and heart of rat. *Metabolism.* 1995;44(9):1185-9.
48. Cittadini A, Mantzoros CS, Hampton TG, Travers KE, Katz SE, Morgan JP, et al. Cardiovascular abnormalities in transgenic mice with reduced brown fat: an animal model of human obesity. *Circulation.* 1999;100(21):2177-83.
49. Harrison SL, Buckley BJR, Rivera-Caravaca JM, Zhang J, Lip GYH. Cardiovascular risk factors, cardiovascular disease, and COVID-19: an umbrella review of systematic reviews. *Eur Heart J Qual Care Clin Outcomes.* 2021;7(4):330-9.
50. All the while hunger continues to be the world's biggest health problem, obesity is on the rise.: The world counts 2024 [Available from: <https://www.theworldcounts.com/challenges/people-and-poverty/hunger-and-obesity/statistics-about-obesity>].
51. Zaromytidou M, Savvatis K. The weight of obesity in hypertrophic cardiomyopathy. *Clinical Medicine.* 2023;23(4):357-63.
52. Singla P, Bardoloi A, Parkash AA. Metabolic effects of obesity: A review. *World J Diabetes.* 2010;1(3):76-88.
53. Betz MJ, Enerbäck S. Human Brown Adipose Tissue: What We Have Learned So Far. *Diabetes.* 2015;64(7):2352-60.
54. Takx RA, Ishai A, Truong QA, MacNabb MH, Scherrer-Crosbie M, Tawakol A. Supraclavicular Brown Adipose Tissue 18F-FDG Uptake and Cardiovascular Disease. *J Nucl Med.* 2016;57(8):1221-5.
55. Pinckard KM, Stanford KI. The Heartwarming Effect of Brown Adipose Tissue. *Mol Pharmacol.* 2022;102(1):460-71.
56. Cabrero À, Alegret M, Sánchez RM, Adzet T, Laguna JC, Carrera MV. Increased Reactive Oxygen Species Production Down-regulates Peroxisome Proliferator-activated  $\alpha$  Pathway in C2C12 Skeletal Muscle Cells\*. *Journal of Biological Chemistry.* 2002;277(12):10100-7.
57. von Essen G, Lindsund E, Cannon B, Nedergaard J. Adaptive facultative diet-induced thermogenesis in wild-type but not in UCP1-ablated mice. *American Journal of Physiology-Endocrinology and Metabolism.* 2017;313(5):E515-E27.
58. Planavila A, Redondo I, Hondares E, Vinciguerra M, Munts C, Iglesias R, et al. Fibroblast growth factor 21 protects against cardiac hypertrophy in mice. *Nat Commun.* 2013;4:2019.
59. Pereira RO, McFarlane SI. The Role of Brown Adipose Tissue in Cardiovascular Disease Protection: Current Evidence and Future Directions. *Int J Clin Res Trials.* 2019;4(2).
60. Harms M, Seale P. Brown and beige fat: development, function and therapeutic potential. *Nature Medicine.* 2013;19(10):1252-63.
61. Jung SM, Sanchez-Gurmaches J, Guertin DA. Brown Adipose Tissue Development and Metabolism. *Handb Exp Pharmacol.* 2019;251:3-36.
62. Fromme T, Klingenspor M. Uncoupling protein 1 expression and high-fat diets. *Am J Physiol Regul Integr Comp Physiol.* 2011;300(1):R1-8.
63. Guo R, Zhang Y, Turdi S, Ren J. Adiponectin knockout accentuates high fat diet-induced obesity and cardiac dysfunction: role of autophagy. *Biochim Biophys Acta.* 2013;1832(8):1136-48.

64. Maillet M, van Berlo JH, Molckentin JD. Molecular basis of physiological heart growth: fundamental concepts and new players. *Nat Rev Mol Cell Biol.* 2013;14(1):38-48.
65. Brady TM. The Role of Obesity in the Development of Left Ventricular Hypertrophy Among Children and Adolescents. *Curr Hypertens Rep.* 2016;18(1):3.
66. Oldfield CJ, Duhamel TA, Dhalla NS. Mechanisms for the transition from physiological to pathological cardiac hypertrophy. *Can J Physiol Pharmacol.* 2020;98(2):74-84.
67. Samak M, Fatullayev J, Sabashnikov A, Zerriouh M, Schmack B, Farag M, et al. Cardiac Hypertrophy: An Introduction to Molecular and Cellular Basis. *Med Sci Monit Basic Res.* 2016;22:75-9.
68. Marian AJ, Braunwald E. Hypertrophic Cardiomyopathy: Genetics, Pathogenesis, Clinical Manifestations, Diagnosis, and Therapy. *Circ Res.* 2017;121(7):749-70.
69. Wang Z, Li L, Zhao H, Peng S, Zuo Z. Chronic high fat diet induces cardiac hypertrophy and fibrosis in mice. *Metabolism.* 2015;64(8):917-25.
70. Ternacle J, Wan F, Sawaki D, Surenaud M, Pini M, Mercedes R, et al. Short-term high-fat diet compromises myocardial function: a radial strain rate imaging study. *European Heart Journal - Cardiovascular Imaging.* 2017;18(11):1283-91.
71. Goetze JP, Bruneau BG, Ramos HR, Ogawa T, de Bold MK, de Bold AJ. Cardiac natriuretic peptides. *Nat Rev Cardiol.* 2020;17(11):698-717.
72. Cabiati M, Raucci S, Liistro T, Belcastro E, Prescimone T, Caselli C, et al. Impact of obesity on the expression profile of natriuretic peptide system in a rat experimental model. *PLoS One.* 2013;8(8):e72959.
73. James SK, Lindahl B, Siegbahn A, Stridsberg M, Venge P, Armstrong P, et al. N-terminal pro-brain natriuretic peptide and other risk markers for the separate prediction of mortality and subsequent myocardial infarction in patients with unstable coronary artery disease: A global utilization of strategies to open occluded arteries (GUSTO)-IV substudy. *Circulation.* 2003;108(3):275-81.
74. Wang TJ, Larson MG, Levy D, Benjamin EJ, Leip EP, Wilson PW, Vasani RS. Impact of obesity on plasma natriuretic peptide levels. *Circulation.* 2004;109(5):594-600.
75. Noordali H, Loudon BL, Frenneaux MP, Madhani M. Cardiac metabolism - A promising therapeutic target for heart failure. *Pharmacol Ther.* 2018;182:95-114.
76. Pascual F, Coleman RA. Fuel availability and fate in cardiac metabolism: A tale of two substrates. *Biochimica et Biophysica Acta (BBA) - Molecular and Cell Biology of Lipids.* 2016;1861(10):1425-33.
77. Ritterhoff J, Young S, Villet O, Shao D, Neto FC, Bettcher LF, et al. Metabolic Remodeling Promotes Cardiac Hypertrophy by Directing Glucose to Aspartate Biosynthesis. *Circ Res.* 2020;126(2):182-96.
78. Pettersen IK, Tusubira D, Ashrafi H, Dyrstad SE, Hansen L, Liu XZ, et al. Upregulated PDK4 expression is a sensitive marker of increased fatty acid oxidation. *Mitochondrion.* 2019;49:97-110.
79. Pettersen IK, Tusubira D, Ashrafi H, Dyrstad SE, Hansen L, Liu X-Z, et al. Upregulated PDK4 expression is a sensitive marker of increased fatty acid oxidation. *Mitochondrion.* 2019;49:97-110.
80. Page AJ, Hatzinikolas G, Vincent AD, Cavuoto P, Wittert GA. The TRPV1 channel regulates glucose metabolism. *Am J Physiol Endocrinol Metab.* 2019;317(4):E667-e76.
81. Knudsen J, Neergaard TB, Gaigg B, Jensen MV, Hansen JK. Role of acyl-CoA binding protein in acyl-CoA metabolism and acyl-CoA-mediated cell signaling. *J Nutr.* 2000;130(2S Suppl):294s-8s.
82. Gabriel-Costa D, Cunha TF, Paixão NA, Fortunato RS, Rego-Monteiro ICC, Barreto-Chaves MLM, Brum PC. Lactate-upregulation of lactate oxidation complex-related genes is blunted in left ventricle of myocardial infarcted rats. *Braz J Med Biol Res.* 2018;51(11):e7660.
83. Cluntun AA, Badolia R, Lettlova S, Parnell KM, Shankar TS, Diakos NA, et al. The pyruvate-lactate axis modulates cardiac hypertrophy and heart failure. *Cell Metab.* 2021;33(3):629-48.e10.
84. Ma XM, Geng K, Wang P, Jiang Z, Law BY-K, Xu Y. MCT4-dependent lactate transport: a novel mechanism for cardiac energy metabolism injury and inflammation in type 2 diabetes mellitus. *Cardiovascular Diabetology.* 2024;23(1):96.

85. Jones TE, Pories WJ, Houmard JA, Tanner CJ, Zheng D, Zou K, et al. Plasma lactate as a marker of metabolic health: Implications of elevated lactate for impairment of aerobic metabolism in the metabolic syndrome. *Surgery*. 2019;166(5):861-6.
86. Ullah MS, Davies AJ, Halestrap AP. The plasma membrane lactate transporter MCT4, but not MCT1, is up-regulated by hypoxia through a HIF-1 $\alpha$ -dependent mechanism. *J Biol Chem*. 2006;281(14):9030-7.
87. Fernandez-Caggiano M, Kamynina A, Francois AA, Prysyzhna O, Eykyn TR, Krasemann S, et al. Mitochondrial pyruvate carrier abundance mediates pathological cardiac hypertrophy. *Nat Metab*. 2020;2(11):1223-31.
88. Bertero E, Maack C. Metabolic remodelling in heart failure. *Nat Rev Cardiol*. 2018;15(8):457-70.
89. Vadvalkar SS, Matsuzaki S, Eyster CA, Giorgione JR, Bockus LB, Kinter CS, et al. Decreased Mitochondrial Pyruvate Transport Activity in the Diabetic Heart: ROLE OF MITOCHONDRIAL PYRUVATE CARRIER 2 (MPC2) ACETYLATION. *J Biol Chem*. 2017;292(11):4423-33.
90. McCommis KS, Kovacs A, Weinheimer CJ, Shew TM, Koves TR, Ilkayeva OR, et al. Nutritional modulation of heart failure in mitochondrial pyruvate carrier-deficient mice. *Nat Metab*. 2020;2(11):1232-47.
91. Bonnefont J-P, Djouadi F, Prip-Buus C, Gobin S, Munnich A, Bastin J. Carnitine palmitoyltransferases 1 and 2: biochemical, molecular and medical aspects. *Molecular Aspects of Medicine*. 2004;25(5):495-520.
92. Stanley WC, Dabkowski ER, Ribeiro RF, Jr., O'Connell KA. Dietary fat and heart failure: moving from lipotoxicity to lipoprotection. *Circ Res*. 2012;110(5):764-76.
93. Czarzasta K, Koperski Ł, Fus Ł, Wojno O, Górnicka B, Cudnoch-Jędrzejewska A. The effects of a high-fat diet on left ventricular fibrosis. *Kardiol Pol*. 2018;76(4):802-4.
94. Martins F, Campos DH, Pagan LU, Martinez PF, Okoshi K, Okoshi MP, et al. High-fat Diet Promotes Cardiac Remodeling in an Experimental Model of Obesity. *Arq Bras Cardiol*. 2015;105(5):479-86.
95. Qin F, Siwik DA, Luptak I, Hou X, Wang L, Higuchi A, et al. The polyphenols resveratrol and S17834 prevent the structural and functional sequelae of diet-induced metabolic heart disease in mice. *Circulation*. 2012;125(14):1757-64, s1-6.
96. Calligaris SD, Lecanda M, Solis F, Ezquer M, Gutiérrez J, Brandan E, et al. Mice long-term high-fat diet feeding recapitulates human cardiovascular alterations: an animal model to study the early phases of diabetic cardiomyopathy. *PLoS One*. 2013;8(4):e60931.
97. Kuivaniemi H, Tromp G. Type III collagen (COL3A1): Gene and protein structure, tissue distribution, and associated diseases. *Gene*. 2019;707:151-71.
98. Cabral-Pacheco GA, Garza-Veloz I, Castruita-De la Rosa C, Ramirez-Acuña JM, Perez-Romero BA, Guerrero-Rodriguez JF, et al. The Roles of Matrix Metalloproteinases and Their Inhibitors in Human Diseases. *International Journal of Molecular Sciences [Internet]*. 2020; 21(24).
99. Wang Y, Jiao L, Qiang C, Chen C, Shen Z, Ding F, et al. The role of matrix metalloproteinase 9 in fibrosis diseases and its molecular mechanisms. *Biomedicine & Pharmacotherapy*. 2024;171:116116.
100. Hayashi D, Kudoh S, Shiojima I, Zou Y, Harada K, Shimoyama M, et al. Atrial natriuretic peptide inhibits cardiomyocyte hypertrophy through mitogen-activated protein kinase phosphatase-1. *Biochemical and Biophysical Research Communications*. 2004;322(1):310-9.
101. Thoonen R, Hindle AG, Scherrer-Crosbie M. Brown adipose tissue: The heat is on the heart. *Am J Physiol Heart Circ Physiol*. 2016;310(11):H1592-605.
102. Chouchani ET, Kazak L, Spiegelman BM. New Advances in Adaptive Thermogenesis: UCP1 and Beyond. *Cell Metab*. 2019;29(1):27-37.
103. Lopaschuk GD, Ussher JR, Folmes CD, Jaswal JS, Stanley WC. Myocardial fatty acid metabolism in health and disease. *Physiol Rev*. 2010;90(1):207-58.
104. Altschul SF, Gish W, Miller W, Myers EW, Lipman DJ. Basic local alignment search tool. *J Mol Biol*. 1990;215(3):403-10.
105. UniProt: the universal protein knowledgebase in 2021. *Nucleic Acids Res*. 2021;49(D1):D480-d9.

*Acknowledgements* – This thesis was supported by Grant PID2021-122941OB-I00 funded by MCIN/AEI/10.13039/501100011033 and by “ERDF A way of making Europe” and Sociedad Española de Cardiología (SEC/FEC-INV-BAS 21/002). I am deeply grateful for Prof. Dr. Anna Planavila (Universitat de Barcelona) as my principal supervisor for the opportunity to join this team and for all the assistance and support in accomplishing this master thesis. I am also thankful for the support from my internal supervisor Prof. Dr. Virginie Bito (Universiteit Hasselt) for sharing her expertise and supporting me during this process. Appreciation is extended to Prof. Dr. Francesc Villaroya (Universitat de Barcelona) for contributing in my research. I would also like to express a special thank you to my daily supervisor Albert Blasco-Roset for teaching and supporting me in the lab. Moreover, ABR helped me with data analysis and writing of the thesis and I thank him for the patience and encouragement. I would also like to thank Artur Navarro for guiding me in the cell culture lab and assisting in data analysis. Profound appreciation is expressed to Tania Quesada-López, Alberto Mestres-Arenas, Marion Peyrou, Francisco Javier Godoy Nieto, and Celia Rupérez for sharing their expertise and answering my questions and Merche Moralis for the technical support in the lab. The Erasmus+ program is acknowledged for facilitating and funding this unforgettable experience. Lastly, I am profoundly grateful for my parents and family's support, encouragement, and sacrifices during this master's thesis.

*Author contributions* – This study was designed by AP and FV. In vivo experiments were performed by ABR. Tissue analysis was carried out by ABR and NS. In vitro experiments were conducted by NS and AN. Data was analyzed by NS. The thesis was written by NS and reviewed by ABR and AP.

SUPPLEMENTARY MATERIAL

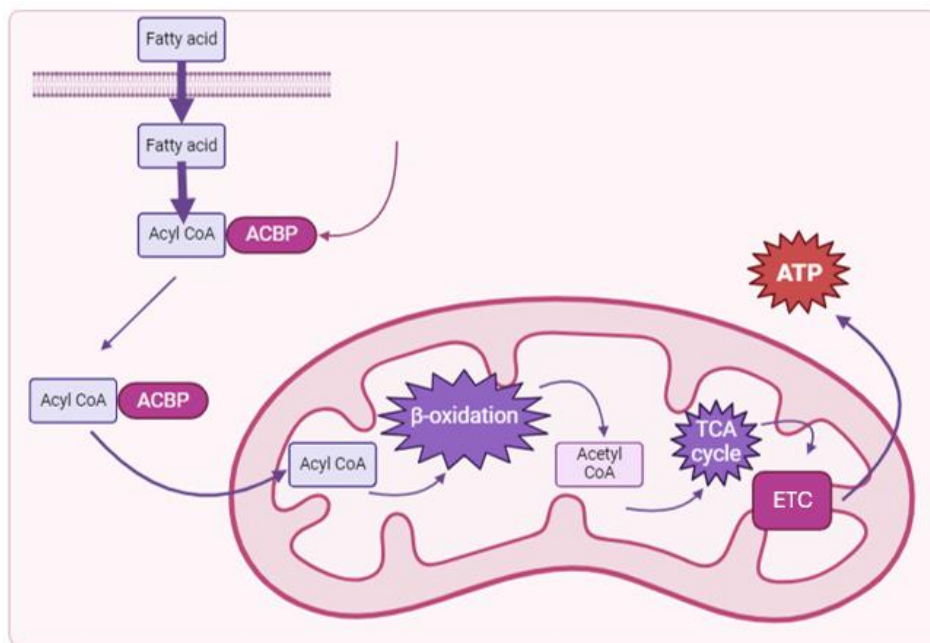
```

      10          20          30          40          50          60
Homo Sapiens: MSQAEFEKAA  EEVRHLKTKP  SDEEMLFIYG  HYKQATVGD  NTERPGMLDF  TGKAKWDAWN
Mus musculus: MSQAEFDKAA  EEVKRLKTQP  TDEEMLFIYS  HFKQATVGDV  NTDRPGLLDL  KGKAKWDSWN
*****:* **:*:*:*:* :*****. *:*****: **:*:*:*: .*****:*

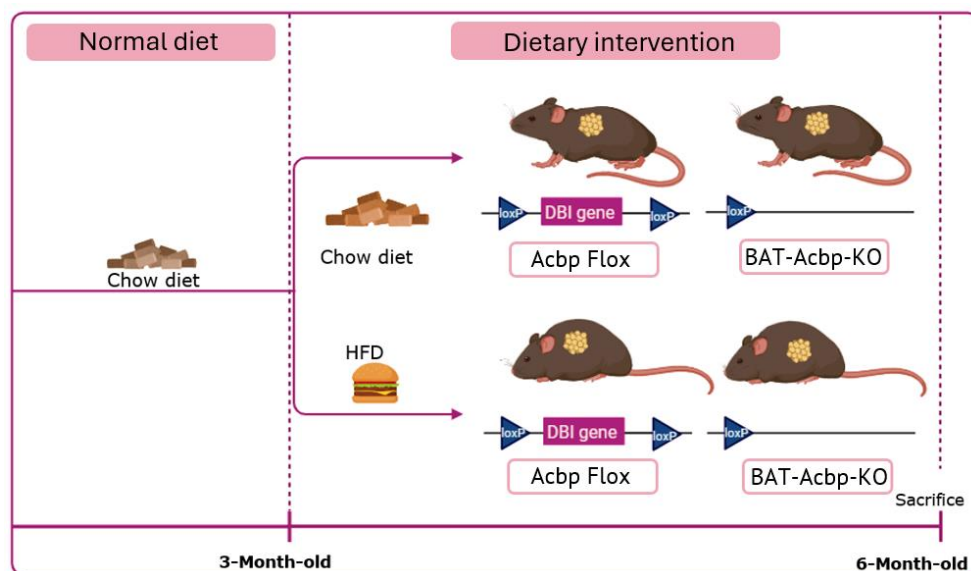
      70          80          87
Homo Sapiens: ELKGTSKEDA  MKAYINKVEE  LKKKYGI
Mus musculus: KLKGTSKESA  MKTYVEKVDE  LKKKYGI
:*****.* **:*:*:*:* *****
*= conserved := conservative .=semi-conservative
Identities: 68/87 (78%) Positives: 80/87(91%) E value: 1e-54

```

**Supplementary Figure 1: ACBP sequence alignment between Homo Sapiens (Uniprot ID: P07108) and Mus Musculus (Uniprot ID: P31786) by using the NCBI BLAST tool (<https://blast.ncbi.nlm.nih.gov/Blast.cgi>) (104, 105). The conserved residues (\*), conservative (:), and semi-conservative (.) residues are displayed. An identity of 78% (68/87), positives of 91% (80/87), and an E-value of 1e-54 was obtained.**



**Supplementary Figure 2: The function of ACBP in lipid metabolism.** Representation of ACBP and its role in transporting Acyl Coenzyme A esters to the mitochondria for β-oxidation. *ATP*, adenosine triphosphate; *β-oxidation*, beta oxidation; *CoA*, Coenzyme A; *ETC*, Electron transport chain; *TCA*, tricarboxylic acid; Figure constructed with Biorender



**Supplementary Figure 3 – Representation of the animal models used and diet interventions.** 3-month-old Acbp Flox and BAT-Acbp-KO mice were subjected to a chow diet or a HFD for a 3 month period before sacrifice and collection of the tissue. *ACBP*, *Acyl-CoA binding protein*; *BAT*, *Brown adipose tissue*; *HFD*, *High fat diet*. *KO*, *Knockout*. Figure constructed with Biorender.

**Supplementary table 1 – Taqman RT-PCR gene expression probes.**

Gene	Reference code
<i>Ppia</i>	Mm 02342430_g1
<i>Dbi (Acbp)</i>	Mm 01286585_g1
<i>Myh6</i>	Mm 00440359_m1
<i>Myh7</i>	Mm 00600555_m1
<i>Col1a1</i>	Mm 00801666_g1
<i>TNF (tnfa)</i>	Mm 00443325_m1
<i>Ccl2</i>	Mm 00441242_m1
<i>Acadm</i>	Mm 00431611_m1
<i>Mpc1</i>	Mm 01316203_g1
<i>Mct4</i>	Mm 00446102_m1
<i>Col3a1</i>	Mm 01254476_m1
<i>Mmp9</i>	Mm 00442991_m1
<i>Nppa</i>	Mm 01255747_g1
<i>Timp1</i>	Mm 00441818_m1
<i>Cpt1b</i>	Mm 00487200_m1
<i>Nppb</i>	Mm 01255770_g1

Reference codes are specific identifiers for the genes used in this study.